scientific reports

Check for updates

OPEN

Nitric oxide induces p53-mediated cell death in human nasal epithelial cells

Shizuki Kamiuezono[1], Sho Kubota[2], Tomoki Tsuchida[2], Nobumasa Takasugi[2] & Takashi Uehara[2]✉

Nitric oxide (NO) is a key signaling molecule that plays a vital role in maintaining homeostasis of physiological processes such as immune responses and neurotransmission. However, excessive NO production during inflammatory responses to infection can lead to cytotoxicity and tissue damage. The nasal epithelial barrier is a crucial first line of immunological defense against viral infections, and it is likely exposed to excessive NO levels during chronic inflammation. Therefore, clarifying the effects of NO on this barrier is thus critical. In this study, we investigated the biological effects of sustained NO exposure on RPMI2650 human nasal epithelial cells. Post-NO exposure transcriptomic analyses revealed significant upregulation of genes involved in the p53 signaling pathway. RT-qPCR analyses confirmed the temporal upregulation of p53 target genes associated with apoptosis and cell cycle regulation. These gene expression changes downregulated cell proliferation and induced cell death. Our findings suggest that excessive NO exposure induces nasal epithelial cell death via the p53 pathway, which over the long term can result in tissue damage and dysfunction under inflammatory conditions. These results provide new insights into how prolonged NO exposure affects the nasal epithelial cells and may contribute to the progression of chronic infectious diseases.

Keywords Nitric oxide, p53, Apoptosis, Cell death, Human nasal epithelial cells

Nitric oxide (NO) is a key endogenous signaling molecule that plays vital roles in a variety of physiological processes, including vasodilation, neurotransmission, and immune responses[1–4]. At physiological levels, NO exerts numerous beneficial effects essential for maintaining homeostasis, such as promoting vasodilation and facilitating memory formation. However, excessive NO production during inflammatory responses to infection can lead to cytotoxicity and tissue damage[5].

In response to cytokine stimulation, phagocytic cells such as macrophages produce NO to inhibit invading bacteria and viruses. Due to its high reactivity, NO contributes to the generation of reactive oxygen species (ROS) that impede pathogen proliferation through DNA and RNA damage, ultimately leading to pathogen eradication[6]. However, overproduction of NO during immune responses can induce oxidative stress, harm healthy cells, and promote chronic inflammation and autoimmune diseases. Inducible nitric oxide synthase (iNOS), which is upregulated by inflammatory cytokines, drives sustained and elevated NO synthesis, thereby potentially contributing to NO-mediated chronic toxicity[7]. NO thus functions as somewhat of a "double-edged sword" due to its dual, context-dependent roles. Disruption of this delicate balance can trigger biological toxicity. NO could play a particularly crucial role in maintaining epithelial barrier function. Inflammatory responses in the airway epithelium can lead to excessive NO production, which may ultimately result in dysfunction of the bronchial epithelial barrier. Similarly, NO overproduction in the skin can induce the death of epidermal cells, thereby compromising structural integrity and disrupting the epithelial barrier[8,9].

The nasal epithelial barrier is a crucial first line of defense against pathogens such as viruses and bacteria and contaminants such as air pollutants. Because the olfactory system is directly exposed to the external environment via the nasal epithelium, the nasal mucosa represents a potential site of inflammation through which pathogens and pollutants can infiltrate the brain[10,11]. SARS-CoV-2 primarily enters the body through the nasal and respiratory pathways, and local inflammation in the olfactory system has been reported in patients exhibiting olfactory impairment[12]. Recent studies have suggested that the inflammation of the nasal mucosal epithelium associated with COVID-19 contributes to prolonged olfactory dysfunction[13,14]. In addition, increased iNOS

[1]Department of Medicinal Pharmacology, Faculty of Pharmaceutical Sciences, Okayama University, Okayama, Japan. [2]Department of Medicinal Pharmacology, Graduate School of Medicine, Dentistry, and Pharmaceutical Sciences, Okayama University, 1-1-1 Tsushima-naka Kita-ku, Okayama 700-8530, Japan. ✉email: uehara-t@okayama-u.ac.jp

expression in COVID-19 patients suggests a potential link between NO signaling and the underlying disease pathology[15].

Based on these observations, we hypothesized that NO exacerbates the effects of infection by compromising the nasal epithelial barrier. However, no previous studies have examined how NO functions within the nasal barrier during infectious diseases. To address this knowledge gap, we employed RPMI2650 human nasal epithelial cells derived from the upper respiratory tract. The primary aim of the study was to elucidate the impact of NO overproduction on nasal epithelial cells and the underlying mechanisms of NO-induced cell death.

Results

NO alters gene expression in RPMI2650 cells

The effects of chronic NO exposure were examined by treating RPMI2650 human nasal epithelial cells with the NO donor *S*-nitrosoglutathione (GSNO) for 72 h. This concentration was selected based on previous reports showing that GSNO within the range of 50-500 μM induces biological response in various cell types[16]. Moreover, inflammatory conditions have been reported to cause local increases in NO concentrations approaching 100 μM[17].

Analysis of cell viability every 24 h using the WST-8 assay revealed that NO progressively suppressed cell proliferation over time (Supplementary Fig. S1a). Staining of dead cells using propidium iodide (PI) and Hoechst 33342 showed a gradual upregulation of cell death with prolonged NO exposure (Supplementary Fig. S1b). These results indicate that long-term NO exposure induces nasal epithelial cell death.

To investigate the molecular mechanisms underlying NO-induced cell death in greater detail, RPMI2650 cells were treated with GSNO for 48 h and then subjected to RNA sequencing analysis, as significant cell death was observed at 48 h (Supplementary Fig. S1). Subsequent transcriptomic analysis of control cells treated with glutathione (GSH) and GSNO-treated cells revealed a large number of differentially expressed genes (DEGs), with 651 upregulated and 150 downregulated genes identified (Figure 1a). The biological significance of the 651 upregulated genes was explored using Gene Ontology (GO) analysis, which showed significant enrichment of GO terms related to the DNA damage response and cell-cycle regulation by p53-class mediators (Figure 1b). The 150 downregulated genes, by contrast, were predominantly associated with DNA replication-dependent chromatin assembly (Figure 1c). Gene Set Enrichment Analysis (GSEA) confirmed the activation of p53 pathway-related genes (Figure 1d). Consistent with these results, Kyoto Encyclopedia of Genes and Genomes (KEGG) pathway enrichment analysis showed the highest degree of enrichment in the p53 signaling pathway (Figure 1e). KEGG Pathview analysis of the p53 signaling pathway (hsa04115) identified a number of genes upregulated by NO treatment (Supplementary Fig. S2). We focused on the apoptosis-related genes BBC3, PMAIP1, PERP, PIDD1, TP53I3, ZMAT3, and CDKN1A. The upregulation of these genes has been suggested to promote stress-induced cell death in various cell types[18,19]. Collectively, these results imply that excessive NO exposure activates p53-dependent signaling pathways associated with cell-cycle regulation and apoptosis in nasal epithelial cells.

NO activates p53 to promote target gene expression

RT-qPCR analysis of the apoptosis- and cell-cycle regulation-related genes listed in Figure 1 was conducted to characterize the changes in expression of these genes over time (24 to 72 h). All of the genes examined were significantly upregulated by GSNO treatment, with most exhibiting an increase in expression over time (Figure 2). These findings suggest that NO induces transcription of these genes via p53 activation, ultimately leading to cell death.

To characterize p53 activation by NO, p53 protein expression was analyzed using Western blotting. Previous research showed that after activation, p53 evades proteasomal degradation and accumulates within cells[20]. In our time-course analysis, a significant increase in p53 protein levels was observed at 3 h after GSNO treatment (Figure 3a). MDM2 functions as a key negative regulator of p53 by modulating its stability and transcriptional activity, whereas p53 in turn transcriptionally induces MDM2, thus forming a negative feedback loop[21]. Consistent with these findings, we found that MDM2 accumulates simultaneously with p53 following NO treatment (Figure 3a). These results suggest that NO activates the p53 pathway, resulting in p53 accumulation and the subsequent induction of downstream targets such as MDM2. This activation of p53 likely represents an early event that initiates the transcription of apoptosis-related genes, ultimately resulting in nasal epithelial cell death.

Our data indicate that NO activates p53 signaling and upregulates apoptosis-related genes. To further verify whether NO-induced cell death involves apoptosis, PARP cleavage was examined using Western blotting after 48 h of GSNO treatment. Significant increases in cleaved PARP were observed, confirming activation of the apoptotic pathway (Supplementary Fig. S3a). In addition, annexin V/PI double staining was performed, in which annexin V stains phosphatidylserine externalized during early apoptosis. A pronounced overlap between annexin V-positive and PI-positive cells was detected, indicating that a substantial fraction of NO-exposed cells underwent apoptosis (Supplementary Fig. S3b, c). These findings demonstrate that apoptosis is a major contributing mechanism to the cell death induced by prolonged NO exposure.

Using the p53 inhibitor pifithrin-α, we also investigated changes in the expression of p53 target genes. Pifithrin-α reportedly inhibits the binding of p53 to DNA by altering its post-translational modification[22]. Consistent with previous reports, we found that p53 protein expression was not affected by pifithrin-α, but MDM2 expression was suppressed (Figure 3b). Results similar to NO treatment were obtained in cells treated with 200 μM hydrogen peroxide (H_2O_2), a positive control for oxidative stress. These results demonstrate that oxidative stress induced p53-mediated cell death. Furthermore, RT-qPCR analysis demonstrated that pifithrin-α significantly suppressed the upregulation of GSNO-induced genes, as previously shown in Figure 2 (Figure 3c). Collectively, these findings suggest that p53 activation is involved in the NO-mediated transcriptional regulation that ultimately leads to nasal epithelial cell death.

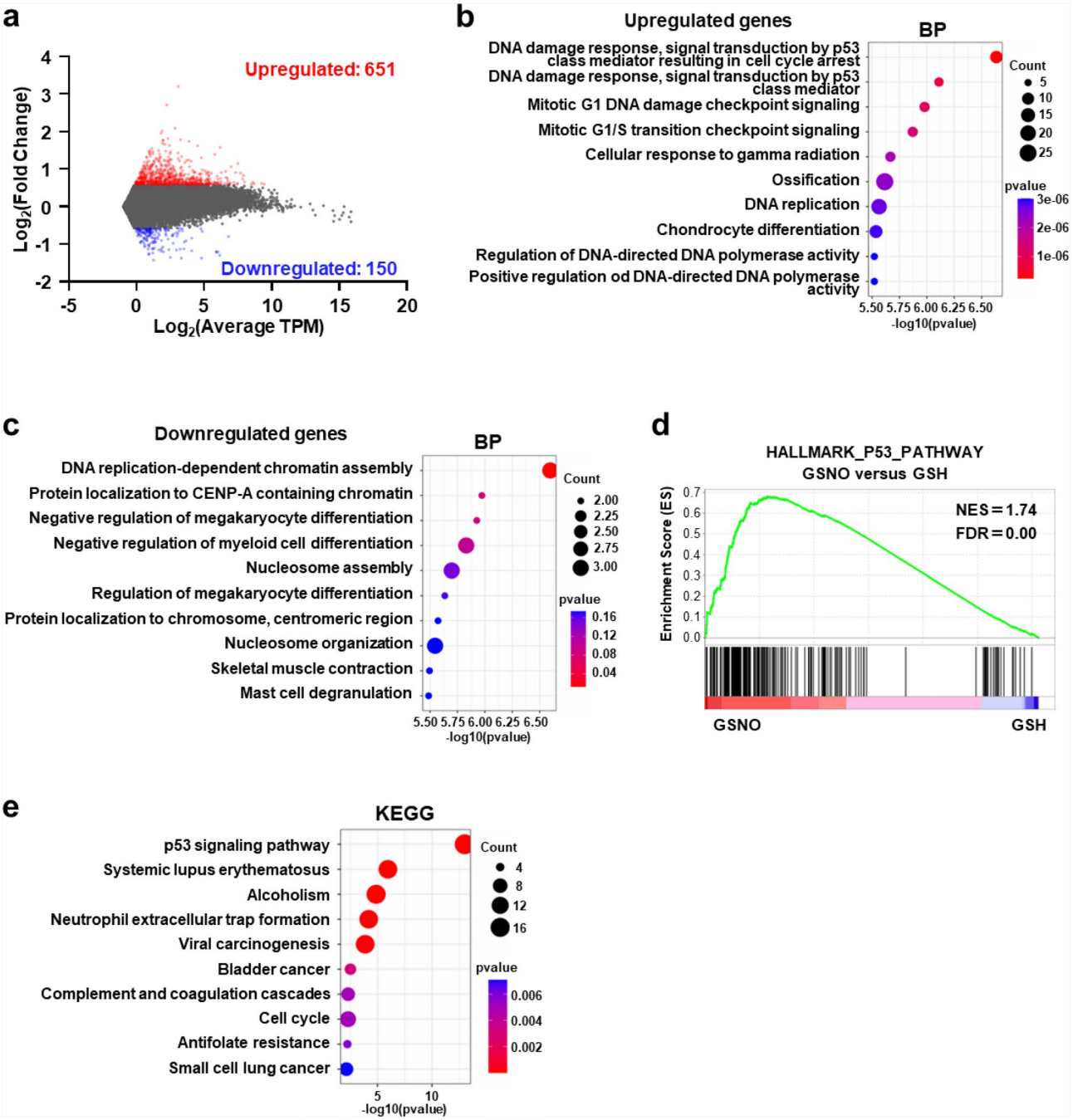

Fig. 1. NO alters gene expression in RPMI2650 cells. **a**) MA plot showing differentially expressed genes (DEGs) in RPMI2650 cells treated for 48 h with 100 µM GSNO or 100 µM GSH. Upregulated genes are shown in red (Transcripts per million (TPM) >0.5, fold-change >1.5), and downregulated genes are shown in blue (TPM <0.5, fold-change <0.67); unaffected genes are shown in gray. RNA-seq was performed once. **b**-**c**) Dot plots showing the results of Gene Ontology (GO) analysis for (**b**) 651 upregulated genes and (**c**) 150 downregulated genes. **d**) Gene set enrichment analysis (GSEA) of the HALLMARK_P53_PATHWAY gene set (https://www.gsea-msigdb.org/gsea/msigdb/human/geneset/HALLMARK_P53_PATHWAY.html). **e**) Dot plots showing the results of KEGG pathway enrichment analysis of the 651 upregulated genes using the KEGG pathway database (https://www.genome.jp/kegg/pathway.html). KEGG pathway data were used in this study with permission from the Kanehisa laboratory for publication.

NO induces the death of RPMI2650 cells via p53 activation

PI and Hoechst 33342 staining was used to determine whether pifithrin-α inhibits NO-induced apoptosis of RPMI2650 cells. Although the proportion of dead cells increased over time following NO exposure (Supplementary Fig. S1b), treatment with pifithrin-α significantly reduced the number of dead cells (Figure 4a).

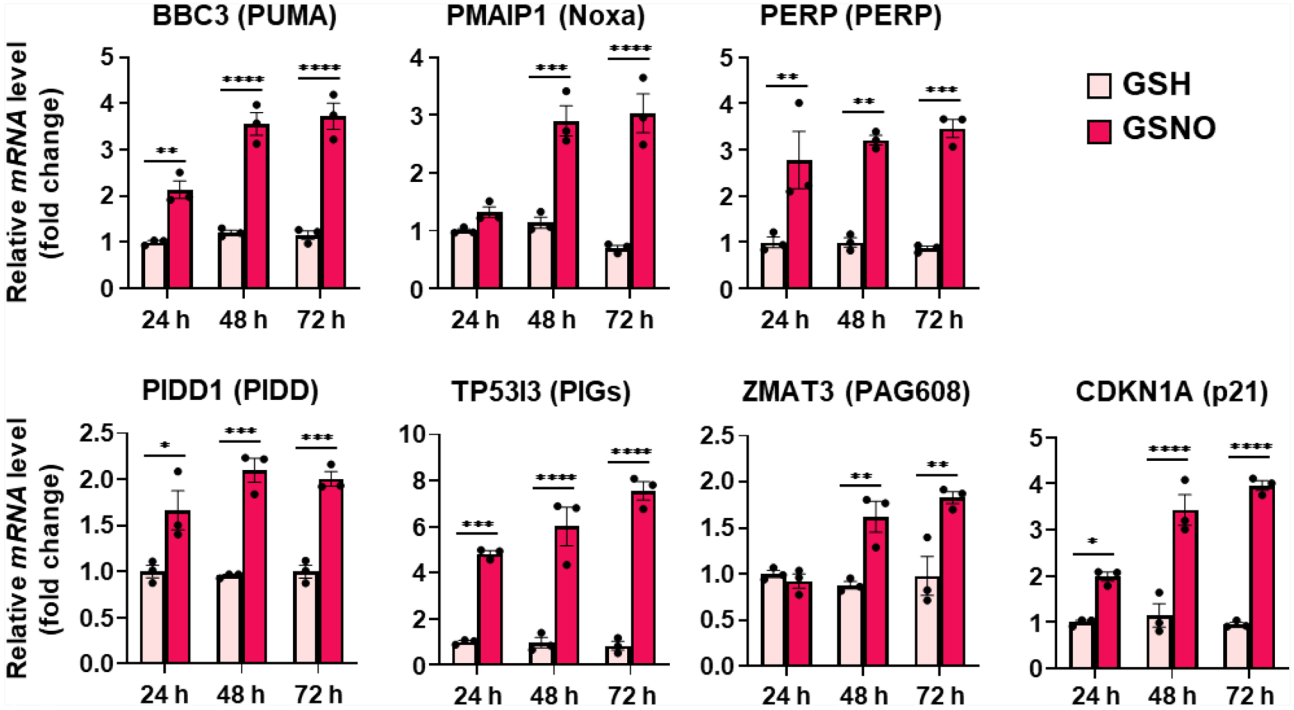

Fig. 2. NO upregulates p53 target genes. RPMI2650 cells were treated with 100 μM GSNO for the indicated times. Expression of the BBC3, PMAIP1, PERP, PIDD1, TP53I3, ZMAT3, and CDKN1A genes was analyzed using RT-qPCR. The relative expression of each gene in the control GSH group is shown in pink, whereas that of cells treated with GSNO is shown in red. The data are expressed as the mean (n=3), *p<0.05, **p<0.01, ***p<0.001, ****p<0.0001 versus control GSH for GSNO-treated cells at the same timepoint. The significance of differences was evaluated using one-way ANOVA with Tukey's multiple comparison test. Three independent experiments were performed.

These results support the hypothesis that p53 activation plays a role in the NO-induced death of nasal epithelial cells.

Discussion

In this study, we investigated the effects of NO exposure on nasal epithelial cells. Transcriptomic analyses revealed that NO upregulates the expression of p53 target genes associated with cell-cycle regulation and apoptosis. Consequently, NO exposure led to the inhibition of cell proliferation and cell death. Furthermore, pharmacological inhibition of p53 suppressed NO-induced cell death. Our results demonstrate that p53 activation is involved in NO-induced changes in gene expression (Figure 4b).

To understand the biological effects of NO, we treated the cells with 100 μM GSNO for 72 h. The experimental conditions used in this study were designed to recapitulate sustained NO exposure in inflammatory conditions. As shown in a previous report, inflammation can locally elevate NO levels to approximately 100 μM[17]. Consistent with this concept, previous studies have shown that cytokine stimulation markedly induces iNOS expression within 24 h and leads to sustained NO production over the following days in human cells[23]. These findings support the notion that inflammatory activation can maintain elevated NO levels for several days, providing a biological basis for the 72 h exposure period used in this study. This experimental condition reflects pathophysiological situations in which prolonged NO production contributes to tissue injury during chronic inflammation, with GSNO serving as a relatively slow releasing NO donor that allowed sustained NO exposure in vitro.

We showed that p53 is one of the major pathways through NO-induced cell death (Figs. 1-4). A notable limitation of this study is that the specific molecular pathways by which NO activates p53 remain incompletely understood, and pharmacological inhibition of p53 only partially rescued NO-induced cell death. Both NO and p53 are key regulators of cellular stress and immune responses, and their interplay contributes to inflammation and cell death[24]. NO is a highly reactive free radical that readily reacts with oxygen or superoxide to generate reactive nitrogen and oxygen species (RNS and ROS), such as peroxynitrite ($ONOO^-$)[25]. These species amplify oxidative and nitrosative stress, causing DNA damage that activates p53 to maintain genomic integrity of the cells. Under prolonged stress, p53 transcriptionally induces pro-oxidant genes, such as *PIG3* (*TP53I3*), thereby promoting apoptosis[26,27]. Thus, NO-induced oxidative stress may indirectly activate p53 via oxidative DNA damage. In addition, NO directly regulates p53 signaling via *S*-nitrosylation. *S*-nitrosylation of MDM2 disrupts its interaction with p53, leading to p53 stabilization[28]. Furthermore, excessive *S*-nitrosylation of p53 may impair

its regulation and weaken antioxidant defenses, ultimately contributing to cellular injury[29]. Further studies are needed to understand the molecular pathways of NO-induced cell death.

Consistent with previous findings, the results of our study demonstrate that NO induces apoptosis of nasal epithelial cells via p53 activation, thereby potentially compromising the nasal epithelial barrier. Barrier disruption can weaken the first line of physiological defense and may increase vulnerability to viral invasion and exacerbate respiratory infections[30]. Recent studies have shown that in patients infected with SARS-CoV-2, iNOS expression is upregulated in response to cytokine stimulation, and this upregulation is correlated with disease severity[15]. COVID-19 is characterized by a cytokine storm that leads to severe tissue damage and long-term consequences[31]. One prominent long-term effect is olfactory dysfunction, which is thought to result from local inflammation in the olfactory system[12,13]. Furthermore, a previous study has proposed that inflammatory cytokines and immune cells can infiltrate the brain via the compromised olfactory epithelium, thereby contributing to neurodegeneration and persistent olfactory dysfunction[13].

During cytokine storms, NO acts as a pro-inflammatory mediator and may also play a role in olfactory dysfunction[5,31]. Interestingly, activation of p53 reportedly plays a central role in cytokine storms associated with SARS-CoV-2 infection[32]. Taken together, these observations raise the possibility that NO contributes to prolonged olfactory dysfunction in COVID-19 patients by promoting inflammation-induced p53 activation. It is therefore important to obtain a more complete understanding of the role of NO in the nasal epithelial barrier under inflammatory conditions. The results of the present study suggest that prolonged NO exposure enhances the expression of apoptosis-related genes via p53 activation, thereby contributing to potential chronic pathological changes. Our findings provide new insights into the mechanism by which NO induces nasal epithelial cell death and may be involved in the continued progression of chronic infectious diseases.

Our experiments were conducted in vitro using RPMI2650 cells, an immortalized nasal epithelial cell line. This cell line provides a practical and reproducible model for mechanistic and transcriptomic studies and has also been widely used to evaluate airway toxicity and epithelial responses to environmental pollutants and inflammatory mediators[33,34]. These applications support the suitability of this model for investigating stress-induced cellular responses. However, our model cannot fully recapitulate the physiological characteristics of the nasal epithelium barrier. Moreover, this study lacked functional assessments of epithelial barrier integrity. Although our transcriptomic data did not reveal significant changes in tight junction-related genes, further functional validation is necessary to determine whether NO exposure directly compromises barrier function. Therefore, it remains unclear whether NO-induced molecular responses, including p53 pathway activation and epithelial cell death, accurately reflect the pathological processes occurring in vivo. Further investigations using primary human nasal epithelial cells or in vivo models would strengthen the physiological and translational relevance of these findings.

Materials and methods

Cell culture

RPMI2650 human nasal septum carcinoma cells were obtained from the Japanese Collection of Research Bioresources Cell Bank (JCRB; JCRB9058). RPMI2650 cells were cultured in Dulbecco's modified Eagle medium (FUJIFILM Wako Pure Chemical Corp., Osaka, Japan) supplemented with 10% (v/v) heat-inactivated fetal bovine serum (Sigma-Aldrich, St. Louis, MO, USA) and 1% penicillin/streptomycin (FUJIFILM Wako Pure Chemical Corp.) at 37°C in a humidified atmosphere containing 5% CO_2/95% air.

Reagents and antibodies

The NO donor GSNO was prepared freshly before use. GSH (FUJIFILM Wako Pure Chemical Corp., #073-02013), pifithrin-α (Tokyo Chemical Industry, Tokyo, Japan, #P2751), and H_2O_2 (FUJIFILM Wako Pure Chemical Corporation, #081-04215) were purchased from the indicated vendors. Antibodies against p53 (Cell Signaling Technology, Danvers, MA, USA, #2524S), MDM2 (Cell Signaling Technology, #86934S), PARP (Cell Signaling Technology, #9542S), Cleaved-PARP (Cell Signaling Technology, #5625S), GAPDH (Cell Signaling Technology, #3683S), anti-rabbit IgG horseradish peroxidase (HRP)-linked F(ab′)2 fragment from donkey (GE Healthcare, Chicago, IL, USA, #NA9340), and anti-mouse IgG HRP-linked F(ab′)2 fragment from sheep (GE Healthcare, #NA9310) were purchased from the indicated vendors.

RNA sequencing and data analysis

RPMI2650 cells were treated with 100 μM GSNO for 48 h. Total RNA was extracted using a Maxwell RSC simply RNA Cell kit (Promega, Madison, WI, USA). RNA quality was assessed using Tapestation 4200 High-Sensitivity RNA tapes (Agilent Technologies, Santa Clara, CA, USA). Extraction and fragmentation of poly(A) RNA from total RNA (100 ng) were performed using the NEBNext Poly(A) mRNA Magnetic Isolation Module (New England BioLabs, Ipswich, MA, USA) and NEBNext Ultra II RNA Library Prep Kit for Illumina (New England BioLabs). Next, cDNAs were synthesized using a NEBNext Ultra II RNA Library Prep Kit for Illumina, followed by adapter tagging using the NEBNext Adaptor (New England BioLabs). Sequencing libraries were prepared by amplifying cDNAs via PCR under the following conditions: 98°C for 30 s, followed by 11 cycles of 98°C for 10 s and 65°C for 75 s. Sequencing of the 50-bp cDNA regions and index sequences was performed using a NovaSeq 6000 SP Reagent kit v1.5 (Illumina, San Diego, CA, USA). All sequence data files were analyzed under default parameters using CLC Genomics Workbench 22.0.1 (Qiagen, GmbH, Hilden, Germany). Quantitative analyses were performed using R software (4.2.3). Minus-Average (MA) plots were generated using GraphPad Prism 10 (GraphPad). GSEA was performed using GSEA software (4.1.0). GO analysis and KEGG pathway enrichment analysis of up- and downregulated DEGs were performed using the clusterProfiler (4.6.2) package[35,36] and org.Hs.eg.db (3.16.0) package as a library. KEGG pathway data were used in this study with permission from the Kanehisa laboratory for publication[37–39].

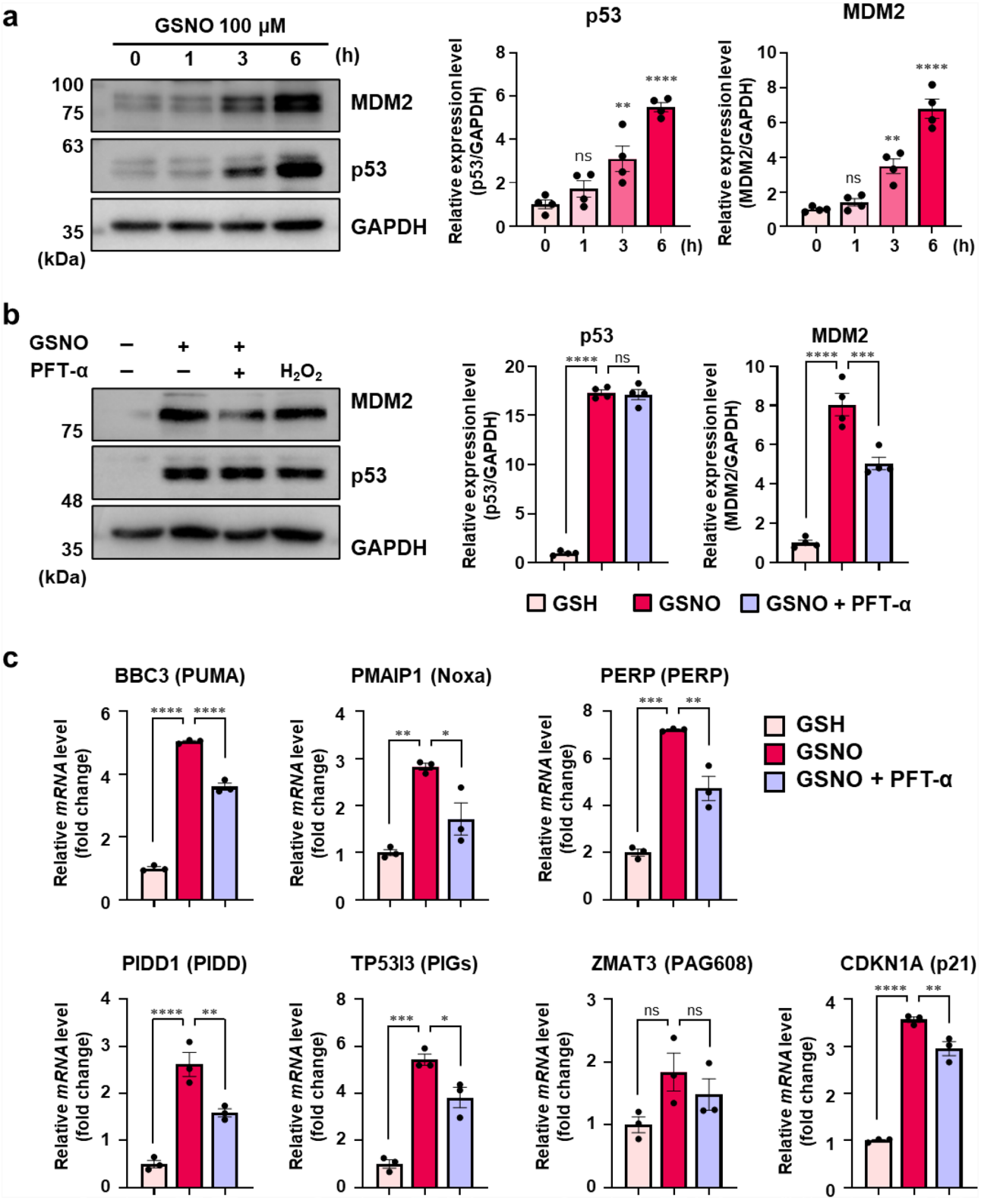

RT-qPCR

RT-qPCR assays were performed as described previously[4]. Total RNA was extracted from RPMI2650 cells using TRI Reagent (Molecular Research Center, Cincinnati, OH, USA), and cDNAs were synthesized from the total RNA using ReverTra Ace RT qPCR Master Mix (TOYOBO, Osaka, Japan) according to the manufacturer's protocol. qPCR was performed using KOD SYBR qPCR Mix (TOYOBO) under the following conditions: 98°C for 2 min, followed by 40 cycles of 98°C for 10 s, 60°C for 10 s, and 68°C for 30 s. The following primer sets were used: human BBC3 5′-GAG CAG GGC AGG AAG TAA CAA-3′ and 5′-GAC CCC ATG CCA AAT TTC ATC C-3′; human PMAIP1 5′-GAG GAA CAA GTG CAA GTA GCT G-3′ and 5′-TCT GCC GGA AGT TCA GTT TGT-3′; human PIDD1 5′-CAC ACA CTT CTC CTG GTA CTG G-3′ and 5′-GCA GAG CGA TGA GGT TCA

◂**Fig. 3**. NO activates p53 to promote target gene expression. a-b) Western blotting analysis of p53 and MDM2 expression (n=3). Uncropped images of the immunoblots are shown in Supplementary Figure S4. a) RPMI2650 cells were treated with 100 µM GSNO for the indicated times. b) RPMI2650 cells were treated with 100 µM GSNO for 6 h; pifithrin-α (10 µM) was added 1 h prior to GSNO treatment. As a positive control for oxidative stress, cells were treated with 200 µM H_2O_2 for 6 h. c) RPMI2650 cells were treated with 100 µM GSNO and 10 µM pifithrin-α for 24 h. Expression of the BBC3, PMAIP1, PERP, PIDD1, TP53I3, ZMAT3, and CDKN1A genes was analyzed using RT-qPCR (n=3). a-c) Relative levels of each parameter in control GSH cells are shown in pink, whereas those in GSNO control cells are shown in red; GSNO and pifithrin-α treatment are shown in purple. Data are expressed as the mean, *p<0.05, **p<0.01, ***p<0.001, ****p<0.0001 for control GSH versus GSNO, and GSNO versus GSNO and pifithrin-α. The significance of differences was evaluated using one-way ANOVA with Tukey's multiple comparison test. Three or four independent experiments were performed.

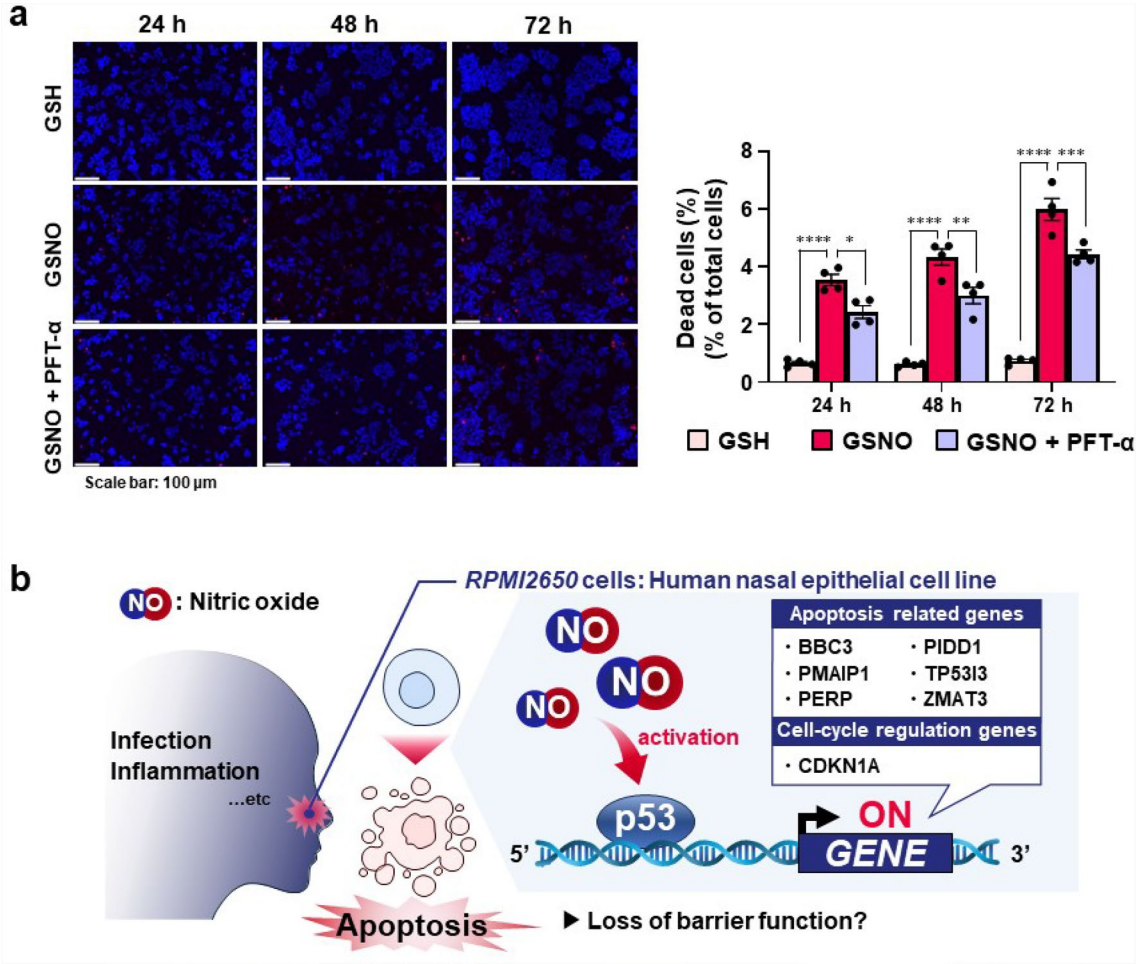

Fig. 4. NO induces apoptosis of RPMI2650 cells via p53 activation. **a**) RPMI2650 cells were treated with 100 µM GSNO for the indicated times; pifithrin-α (10 µM) was added 1 h prior to GSNO treatment. Dead cells were quantified by PI and Hoechst 33342 staining. PI (red) was used as a marker of dead cells and Hoechst 33342 (blue) as a marker of nuclei. The ratio (%) of dead to live cells was calculated based on the number of PI-positive cells relative to Hoechst-positive cells. Control GSH is shown in pink, GSNO is shown in red, and combined GSNO and pifithrin-α treatment is shown in purple. Data are expressed as the mean (n=4), *p<0.05, **p<0.01, ***p<0.001, ****p<0.0001 for control GSH versus GSNO, and GSNO versus GSNO and pifithrin-α at the same time points. The significance of differences was evaluated using one-way ANOVA with Tukey's multiple comparison test. Four independent experiments were performed. **b**) Excessive NO produced during infection and inflammatory responses activates p53 in human nasal epithelial cells (RPMI2650), inducing the expression of p53 target genes related to cell-cycle regulation and apoptosis, ultimately leading to cell death. This process may contribute to the loss of barrier function in the nasal epithelium.

CA-3′; human PERP 5′-GGG CTG AGA AAC CAC CTG AA-3′ and 5′-GCC ACT TAG CAT GTC TGG CT-3′; human TP53I3 5′-GAA ATT CAC CAA AGG TGC TGG A-3′ and 5′-CCA GGC AGT TGA CGT TCT TC-3′; human ZMAT3 5′-TGG CGG AAG CTC AGA GTA AC-3′ and 5′-GGA TTG AAG TAA GGA CCT GCT GA-3′; human CDKN1A 5′-AGT CAG TTC CTT GTG GAG CC-3′ and 5′-GAC ATG GCG CCT CCT CTG-3′; human ACTB 5′-TCA CCC ACA CTG TGC CCA TCT ACG A-3′ and 5′-CAG CGG AAC CGC TCA TTG CCA CTG G-3′. Gene expression data were quantified via the 2-ΔΔCt relative quantification method, using ACTB for normalization.

Assessment of cell proliferation

RPMI2650 cells were exposed to GSNO (100 μM). At 24-h intervals, the culture medium was completely exchanged with fresh medium, and reagents were re-added. Cells were stained with Hoechst 33342 (10 μM diluted in PBS; Sigma-Aldrich) and PI (10 μg/mL diluted in PBS; Sigma-Aldrich) for 30 min at 37°C. Cells were counted under a BZ-810 fluorescence microscope (Keyence, Osaka, Japan) using ImageJ software. Cell proliferation was evaluated using a Cell Counting Kit-8 (Dojindo, Kumamoto, Japan), and cell proliferation was assessed by measuring the optical density of cultures at 450 nm.

Assessment of apoptosis

Apoptosis was evaluated using the Annexin V-FITC Apoptosis Detection Kit (Nacalai Tesque, Kyoto, Japan). The culture medium was replaced with 1×Binding Buffer supplied with the kit. Cells were stained with 5 μL annexin V-FITC, Hoechst 33342 (10 μM diluted in PBS; Sigma-Aldrich) and PI (10 μg/mL diluted in PBS; Sigma-Aldrich) for 15 min at 37°C. Cells were counted under a BZ-810 fluorescence microscope (Keyence, Osaka, Japan) using ImageJ software.

Western blotting

Western blotting was performed as previously described[40]. Whole-cell protein was quantified using a TaKaRa BCA protein assay kit (TaKaRa) according to the manufacturer's protocol. Total protein was then boiled in 1× Laemmli SDS sample buffer (62.5 mM Tris-HCl [pH 6.8], 5% 2-mercaptoethanol, 2% SDS, and 10% glycerol) for 5 min. Proteins were separated using sodium dodecyl sulfate-polyacrylamide gel electrophoresis and transferred onto polyvinylidene difluoride membranes. The membranes were then blocked with 7.5% bovine serum albumin in Tris-buffered saline containing 0.1% Tween-20 (TBS-T) for 1 h at room temperature and incubated with anti-p53 (1:5000), anti-MDM2 (1:5000), anti-PARP (1:5000), anti-cleaved PARP (1:5000) or anti-GAPDH (1:10000) antibodies at 4°C overnight. The membranes were then washed five times with TBS-T and incubated with HRP-conjugated secondary antibodies (1:25000). The membranes were washed again five times with TBS-T, and antibody-reactive bands were visualized using ImmunoStar LD (FUJIFILM Wako Pure Chemical Corp.) and detected using the ChemiDoc XRS+ System (Bio-Rad). Band intensity on Western blots was quantified using ImageJ software (ver. 1.54d).

Statistical analysis

Data are expressed as the mean ± standard error of the mean. All statistical analyses were performed using GraphPad Prism software, version 10 (GraphPad). The significance of differences was determined using one-way analysis of variance (ANOVA) with Tukey's multiple comparisons test. Statistical significance was set at $p<0.05$. RNA-seq and subsequent transcriptomic analyses were performed once (n=1) as an exploratory dataset to identify NO-responsive genes. All other experiments were independently repeated at least three times, and the number of biological replicates (n) is indicated in each figure legend.

Data availability

RNA sequencing data were deposited in the DDBJ (https://ddbj.nig.ac.jp/search/en) under accession number PRJDB35845.

Received: 16 September 2025; Accepted: 17 February 2026
Published online: 20 February 2026

References

1. Uehara, T. et al. *S*-nitrosylated protein-disulphide isomerase links protein misfolding to neurodegeneration. *Nature* **441**, 513–517. https://doi.org/10.1038/nature04782 (2006).
2. Nakato, R. et al. Regulation of the unfolded protein response via *S*-nitrosylation of sensors of endoplasmic reticulum stress. *Sci. Rep.* **5**, 14812. https://doi.org/10.1038/srep14812 (2015).
3. Numajiri, N. et al. On–off system for PI3-kinase–Akt signaling through *S*-nitrosylation of phosphatase with sequence homology to tensin (PTEN). *Proc. Natl. Acad. Sci. U. S. A.* **108**, 10349–10354. https://doi.org/10.1073/pnas.1103503108 (2011).
4. Okuda, K. et al. Pivotal role for S-nitrosylation of DNA methyltransferase 3B in epigenetic regulation of tumorigenesis. *Nat. Commun.* **14**, 621. https://doi.org/10.1038/s41467-023-36232-6 (2023).
5. Sharma, J. N., Al-Omran, A. & Parvathy, S. S. Role of nitric oxide in inflammatory diseases. *Inflammopharmacology* **15**, 252–259. https://doi.org/10.1007/s10787-007-0013-x (2007).
6. Bogdan, C. Nitric oxide and the immune response. *Nat. Immunol.* **2**, 907–916. https://doi.org/10.1038/ni1001-907 (2001).
7. Cinelli, M. A., Do, H. T., Miley, G. P. & Silverman, R. B. Inducible nitric oxide synthase: Regulation, structure, and inhibition. *Med. Res. Rev.* **40**, 158–189. https://doi.org/10.1002/med.21599 (2020).
8. Daniela, B.-G., Thomas, R. & Kolb-Bachofen, V. Nitric oxide in human skin: Current status and future prospects. *J. Invest. Dermatol.* **110**, 1–7. https://doi.org/10.1046/j.1523-1747.1998.00084.x (1998).
9. Ikeyama, K., Fuziwara, S. & Denda, M. Topical application of neuronal nitric oxide synthase inhibitor accelerates cutaneous barrier recovery and prevents epidermal hyperplasia induced by barrier disruption. *J. Invest. Dermatol.* **127**, 1713–1719. https://doi.org/10.1038/sj.jid.5700742 (2007).

10. Tonelli, L. H. & Postolache, T. T. Airborne inflammatory factors: "From the nose to the brain". *Front. Biosci. (Schol. Ed.)* **2**, 135–152 (2010).
11. Lafever, B. J. & Imamura, F. Effects of nasal inflammation on the olfactory bulb. *J. Neuroinflammation* **19**, 294. https://doi.org/10.1186/s12974-022-02657-x (2022).
12. Butowt, R., Bilinska, K. & Von Bartheld, C. S. Olfactory dysfunction in COVID-19: New insights into the underlying mechanisms. *Trends Neurosci.* **46**, 75–90. https://doi.org/10.1016/j.tins.2022.11.003 (2023).
13. Chen, S. & Wang, S. The immune mechanism of the nasal epithelium in COVID-19–related olfactory dysfunction. *Front. Immunol.* **14**, 1045009. https://doi.org/10.3389/fimmu.2023.1045009 (2023).
14. Gamage, A. M. et al. Human nasal epithelial cells sustain persistent SARS-CoV-2 infection in vitro, despite eliciting a prolonged antiviral response. *mBio* **13**, e0343621. https://doi.org/10.1128/mbio.03436-21 (2022).
15. Gelzo, M. et al. Inducible nitric oxide synthase (iNOS): Why a different production in COVID-19 patients of the two waves?. *Viruses* **14**, 534. https://doi.org/10.3390/v14030534 (2022).
16. Zhang, Y. et al. *S*-nitrosylation of the Peroxiredoxin-2 promotes *S*-nitrosoglutathione-mediated lung cancer cells apoptosis via AMPK-SIRT1 pathway. *Cell Death Dis.* **10**, 329. https://doi.org/10.1038/s41419-019-1561-x (2019).
17. Joo, T. et al. Inhibition of nitric oxide production in LPS-stimulated RAW 264.7 cells by stem bark of *Ulmus pumila* L. *Saudi J. Biol. Sci.* **21**, 427–435. https://doi.org/10.1016/j.sjbs.2014.04.003 (2014).
18. Polyak, K., Xia, Y., Zweier, J. L., Kinzler, K. W. & Vogelstein, B. A model for p53-induced apoptosis. *Nature* **389**, 300–305. https://doi.org/10.1038/38525 (1997).
19. Aubrey, B. J., Kelly, G. L., Janic, A., Herold, M. J. & Strasser, A. How does p53 induce apoptosis and how does this relate to p53-mediated tumour suppression?. *Cell Death Differ.* **25**, 104–113. https://doi.org/10.1038/cdd.2017.169 (2018).
20. Lavin, M. F. & Gueven, N. The complexity of p53 stabilization and activation. *Cell. Death. Differ* **13**, 941–950. https://doi.org/10.1038/sj.cdd.4401925 (2006).
21. Kubbutat, M. H. G., Jones, S. N. & Vousden, K. H. Regulation of p53 stability by Mdm2. *Nature* **387**, 299–303. https://doi.org/10.1038/387299a0 (1997).
22. Zhu, J., Singh, M., Selivanova, G. & Peuget, S. Pifithrin-α alters p53 post-translational modifications pattern and differentially inhibits p53 target genes. *Sci. Rep.* **10**, 1049. https://doi.org/10.1038/s41598-020-58051-1 (2020).
23. Ding, M. et al. Inducible nitric-oxide synthase and nitric oxide production in human fetal astrocytes and microglia. *J. Biol. Chem.* **272**, 11327–11335. https://doi.org/10.1074/jbc.272.17.11327 (1997).
24. Meßmer, U. K., Ankarcrona, M., Nicotera, P. & Brüne, B. p53 expression in nitric oxide-induced apoptosis. *FEBS Lett.* **355**, 23–26. https://doi.org/10.1016/0014-5793(94)01161-3 (1994).
25. Brüne, B. The intimate relation between nitric oxide and superoxide in apoptosis and cell survival. *Antioxid. Redox Signal.* **7**, 497–507. https://doi.org/10.1089/ars.2005.7.497 (2005).
26. Sagiv, A. et al. P53 in bronchial club cells facilitates chronic lung inflammation by promoting senescence. *Cell. Rep.* **22**, 3468–3479. https://doi.org/10.1016/j.celrep.2018.03.009 (2018).
27. He, W., Tang, M., Wu, X., Mu, X. & Nie, X. The role of p53 in regulating chronic inflammation and PANoptosis in diabetic wounds. *Aging Dis.* **16**, 373–393. https://doi.org/10.14336/ad.2024.0212 (2024).
28. Schonhoff, C. M., Daou, M.-C., Jones, S. N., Schiffer, C. A. & Ross, A. H. Nitric oxide-mediated inhibition of Hdm2-p53 binding. *Biochemistry* **41**, 13570–13574. https://doi.org/10.1021/bi026262q (2002).
29. Baldelli, S. & Ciriolo, M. R. Altered S-nitrosylation of p53 is responsible for impaired antioxidant response in skeletal muscle during aging. *Aging* **8**, 3450–3467. https://doi.org/10.18632/aging.101139 (2016).
30. Loxham, M., Davies, D. E. & Blume, C. Epithelial function and dysfunction in asthma. *Clin. Exp. Allergy* **44**, 1299–1313. https://doi.org/10.1111/cea.12309 (2014).
31. Ye, Q., Wang, B. & Mao, J. The pathogenesis and treatment of the `cytokine storm' in COVID-19. *J. Infect.* **80**, 607–613. https://doi.org/10.1016/j.jinf.2020.03.037 (2020).
32. Milani, D. et al. P53/NF-kB balance in SARS-CoV-2 infection: From OMICs, genomics and pharmacogenomics insights to tailored therapeutic perspectives (COVIDomics). *Front. Pharmacol.* **13**, 871583. https://doi.org/10.3389/fphar.2022.871583 (2022).
33. Salib, R. J., Lau, L. C. & Howarth, P. H. The novel use of the human nasal epithelial cell line RPMI 2650 as an *in vitro* model to study the influence of allergens and cytokines on transforming growth factor-β gene expression and protein release. *Clin. Exp. Allergy* **35**, 811–819. https://doi.org/10.1111/j.1365-2222.2005.02258.x (2005).
34. Wang, H. et al. Three-dimensional cultured human nasal epithelial cell model for testing respiratory toxicity and neurotoxicity of air pollutants. *Environ. Sci. Technol.* **59**, 6452–6463. https://doi.org/10.1021/acs.est.4c13205 (2025).
35. Yu, G., Wang, L.-G., Han, Y. & He, Q.-Y. ClusterProfiler: An R package for comparing biological themes among gene clusters. *OMICS* **16**, 284–287. https://doi.org/10.1089/omi.2011.0118 (2012).
36. Kubota, S. et al. Chromatin modifier Hmga2 promotes adult hematopoietic stem cell function and blood regeneration in stress conditions. *EMBO J.* **43**, 2661–2684. https://doi.org/10.1038/s44318-024-00122-4 (2024).
37. Kanehisa, M., Furumichi, M., Sato, Y., Matsuura, Y. & Ishiguro-Watanabe, M. KEGG: Biological systems database as a model of the real world. *Nucleic Acids Res.* **53**, D672–D677. https://doi.org/10.1093/nar/gkae909 (2025).
38. Kanehisa, M. Toward understanding the origin and evolution of cellular organisms. *Protein Sci.* **28**, 1947–1951. https://doi.org/10.1002/pro.3715 (2019).
39. Kanehisa, M. & Goto, S. KEGG: Kyoto Encyclopedia of Genes and Genomes. *Nucleic Acids Res.* **28**, 27–30. https://doi.org/10.1093/nar/28.1.27 (2000).
40. Tsuchida, T. et al. Epigenetic regulation of CXC chemokine expression by environmental electrophiles through DNA methyltransferase inhibition. *Int. J. Mol. Sci.* **25**, 11592. https://doi.org/10.3390/ijms252111592 (2024).

Acknowledgements

We thank Kotoe Sueyoshi and Eriko Nishimura for technical assistance.

Author contributions

T.U. conceived and designed the study. S.K. (Shizuki Kamiuezono) acquired and initially analyzed the data. S.K. (Shizuki Kamiuezono), S.K. (Sho Kubota), and T.T. conducted further analyses. S.K. (Shizuki Kamiuezono) drafted the manuscript. S.K. (Sho Kubota) and N.T. substantively revised the manuscript. All authors approved the submitted version.

Funding

This research was funded by grants-in-aid for Challenging Exploratory Research (22K19380 to T.U.) and Scientific Research (A) (24H00678 to T.U.) from the Ministry of Education, Culture, Sports, Science and Technology (MEXT) of Japan. Funding was also provided by the Smoking Research Foundation (to T.U.) and the JSPS Program for Forming Japan's Peak Research Universities (J-PEAKS) (JPJS00420230010).

Declarations

Competing interests
The authors declare no competing interests.

Additional information
Supplementary Information The online version contains supplementary material available at https://doi.org/10.1038/s41598-026-40908-6.

Correspondence and requests for materials should be addressed to T.U.

Reprints and permissions information is available at www.nature.com/reprints.

Publisher's note Springer Nature remains neutral with regard to jurisdictional claims in published maps and institutional affiliations.